2002 BELTWIDE COTTON CONFERENCES, ATLANTA, GA – JANUARY 8-12

MODELING AND ANALYSIS OF POLYMER AND AIR FLOW CONFIGURATIONS IN NONWOVENS INDUSTRY

A. Mukhopadhyay, J. Sun, A. Troshko and R.O. Prasad
FLUENT Incorporated
Lebanon, NH

Abstract

Computational Fluid Dynamics (CFD) is a new tool that is a significantly time and cost saving for analysis of most equipment and processes of the major NW fabric making processes. Application of CFD includes product design, process design optimization, scale-up as well as troubleshooting. This paper will summarize a few specific applications from the fiber manufacturing and NW industry. These are transient analysis of turbulent flow of air delivery systems in Spun-Bond NW fabric manufacturing; and the Melt-blown dies using advanced turbulent model, Large Eddy Simulation (LES) in the CFD tool from FLUENT. Also presented are the simulation results of airflow and fiber accumulation in a Fluff Pad Machine. This study involved use of another advanced model called Discrete Phase Model (DPM) to track individual fiber elements.

Introduction

Technology trend relating to most of the manufacturing issues in the non-woven industry demands identification and control of macro- and microscopic effects of various process parameters. Experimental understanding of these processes is significantly contributory in furthering the technology. Product variety, quality, consistency, in-service life, economics and tailored properties are some of those issues that are estimated, developed and refined through experiments. Nevertheless, experimental modeling and analysis involve significant preparation, man-hours, cost and infrastructure. Moreover, for micro-scale product manufacturing, experimental intrusion often poses the difficulty of inadvertent manipulation of the operating conditions. Computational methods, on the other hand, provide a very cost-effective set of tools that results in a much faster return of the investment, which in itself, is significantly lower than any standard experimental set up. Additionally, such a computational tool can be very effectivelyused to simulate and study a variety of processes and equipment with very little effort from the user. One of the major advances of computational techniques is the ability to reproduce experimental observations under comparable configurations for a large number of processes. They also provide plausible explanations that are otherwise unavailable due to inherent limitations of the concurrent experimental capabilities.

The capabilities of computational techniques include analysis of flow and heat transfer of a variety of processes and equipment:

- **Polymers:** extruders, gear pumps, spinneret, coat-hanger die analysis, fiber spinning,
- **Air flow:** slot attenuator design, diffuser, suction-box designs, melt-blown die-design, air-laid and water-laid system analysis, fluff lay-down on pad making machines, blowers, pumps, and compressors.

Unlike the chemical and polymer industries, computational techniques, more specifically, Computational Fluid Dynamics (CFD) is relatively new in the NonWovens (NW) industry. In the last couple of years, CFD has received formal acceptance across a number of NW industry members and is gaining momentum primarily due to the quick turn around time and less resource involvement.

All these studies were performed using the CFD tools from FLUENT. CFD involves methods to solve the mass, momentum, energy, and constitutive equations along with appropriate material properties and boundary conditions over discretized control volumes representing the domain of analysis. In particular current tools use the well-established Finite Volume Method (FVM). The computational tool was extensively tested and validated before employing for the studies reported in this paper.

As shown in Figure 1, most of the equipment and processes of the two major NW fabric making processes are suitable for product design, process design optimization, as well as troubleshooting using CFD. This paper will summarize a few specific applications from the fiber manufacturing and NW industry, in general:

- Large Eddy Simulation (LES) of Air delivery system in Spun-Bond NW fabric manufacturing
- LES Analysis of Melt-blown Dies
- Analysis of Air Flow and Fiber Accumulation in a Fluff Pad Machine

Simulation of Air Delivery Systems in Spun-Bonding Processes

Airflow plays a significant role in determining the fabric quality in the nonwoven fabric manufacturing processes. A defect-free nonwoven web manufactured using wet-laid or air-laid system requires near perfect distribution of air jets as much as the polymer conditions to attain the designed conditions for optimum entanglement, size distribution, and overall fabric quality. 'Logs' or 'sticks' (bundles of fibers with aligned cut ends that are never dispersed) may be formed due to a gross under-agitation of fibers during their initial dispersion in the surrounding fluid. 'Ropes' may be formed when fibers encounter a vortex that is about the same size as the fiber length. In Spun Bond (SB) systems, airflow plays several important roles:

- A 'cold air stream' cools continuous fibers leaving the spinneret. The characteristics of cold air streams can have a significant impact on the fiber properties.
- High-speed airflow (with Mach number ~1.0) is used in the fiber drawing process.
- Turbulence in the airflow is utilized to obtain desired Machine-Direction to Cross-Direction (MD/CD) strength ratio.

Understanding of fluid flow characteristics is essential for designing nonwoven fabric manufacturing systems. Airflow configurations involved in nonwoven fabric manufacturing are highly turbulent. Computational simulation of industrial turbulent fluid flows involves solution of the Reynolds-Averaged Navier-Stokes equations (RANS). The RANS approach gives time-averaged flow field information. This is similar to the state-of-the-art experimental techniques as well. The air speed being orders of magnitude higher than the polymer speed inside the die, the time-scale to observe the transients in the fibers is disparate to that of the airflow. Hence, the concentrated effort to investigate polymer-fiber behavior unintentionally limits the airflow characterization to its time-average behavior. Although the time-averaged flow field information is very valuable for many applications (e.g. for determining the cooling rate of fibers), the time-dependent, unsteady character of the flow field plays pivotal role in determining the uniformity of the fiber lay-down process as well as the size distribution of the fibers. The uniformity of fiber lay-down process is directly connected to the physical characteristics and appearance of nonwoven materials. This turbulent unsteadiness of the flow field can be simulated using an advanced turbulence model, the Large Eddy Simulation (LES) approach, that is available in FLUENT software.

Primary Air Flow System Design

The primary airflow system in SB units involves use of very high velocity air (often supersonic). Air is pumped into the slot from a compressed air system. Appropriate designs of the primary airflow systems can result in significant energy savings. To demonstrate the applicability of the CFD analysis for designing primary airflow systems, a primary airflow system with an inlet pressure of 45 psig is considered. Figures 2 and 3 show Mach number contours and velocity vectors in the domain predicted based on the CFD solution. These results demonstrrate the capability of the CFD code to capture flow separation in presence of blunt edges. It is worthwhile to highlight that the separation process is augmented due to the compressibility effects of the highly pressurized in-flow.

Free Jet Flows

The distance between the die exit plane and the forming web as well as the flow pattern therein, have important influences on the fiber laydown process and hence the quality (e.g., fiber orientation, and mechanical properties) of the nonwoven material. By design, this jet flow is unconfined. Thus, it allows significant entrainment of environmental air and produces large scale eddies as the flow decelerates and approaches the web. From the fiber-laydown point of view, the important aspects of the jet expansion include:

1. The acceleration in the potential core and subsequent expansion
2. The formation of large scale eddies at the boundary of the jet and the surrounding air; and most importantly,
3. Momentum exchange between air and the polymer leading to the deceleration of the jet and attenuation and acceleration of the polymer-fiber

Some of the equipment parameters are crucial in achieving the right operating conditions. These are the Die-to-Collector-Distance (DCD), the jet-width at the die opening, and the fluid and thermodynamic properties of air and the polymer.

The characteristics of jet spreading and deceleration are a function of the length-to-width ratio (L/W) of the jet, where the length L is the distance between the forming web and the exit of the slot, and W is the width at the slot exit, as shown in Figure 4. For example, two different jets with different exit widths W will appear similar in jet spreading and velocity reduction when they are plotted on the common basis of the non-dimensional parameter L/W. This is depicted in Figure 4. Figures 5 and 6 show time-averaged and instantaneous velocity vectors in a planar jet as simulated using the RANS and LES models.

The spreading of the jet shown in Figures 4 and 5 is a time-average characterization. Actually the jet boundary is very unsteady where large scale eddies are formed by the viscous shear between the high velocity jet and the quiescent surrounding air (as shown in Figure 6). If the motion of the eddies in Figure 6 is averaged over time then the gradual spreading profile of the jet is obtained as depicted in Figures 4 and 5. Since in reality, the large scale eddy motions are present, they have a substantial impact on the web formation because they entrain fibers before they hit the web and eddies can also impact the web and disturb material already laid down on the web. These latter effects can contribute to the blotchy appearance of the nonwoven material.

Finally, the average jet velocity needs to drop below the fiber linear velocity in order for the fibers to be able to weave and twist in a random manner prior to laydown. At what distance this occurs above the web will have an influence on the quality of the laydown process.

All of the above effects need to be taken into account when adjusting the design of the slot hardware and how it is operated. For example, if the slot exit width W is increased (while maintaining the same slot exit velocity) without also increasing the length L, then L/W ratio is reduced and the average velocity at the web will be increased. Such would have detrimental effects by increasing the strength and velocity at which large scale eddies hit the web and also reducing the distance to the web at which the average jet velocity drops below the fiber linear velocity. This latter effect would reduce the amount of time and distance the fibers can randomly weave and twist prior to laydown.

Diffuser Designs

Reduction of air velocity in the slot can also be accomplished using a gradually diffusing passage. However, an improperly designed diffusing passage can result in large-scale eddies in the flow.

Different regimes of a two-dimensional planar diffuser as obtained from experimental data are shown in Figure 7. Based on the values of diffuser exit to inlet area ratio and the ratio of diffuser length to diffuser inlet width, the flow field in the diffuser will fall under different regimes.

Figures 8 shows the type of flow fields that are obtained in an unseparated diffuser, a diffuser with transient stall as well as a diffuser with fully stalled conditions. These results are obtained using the LES models available in FLUENT CFD software. In particular, the LES approach helps in simulating the transient flow features, which are very important in determining the quality of the fabric produced.

Simulation of Air Delivery Systems in Melt-Blowing Processes

In the melt-blowing process, the polymer is extruded through a die nosepiece at an elevated extrusion temperature to form filaments. These filaments are then attenuated by a hot air stream that is supplied through the air manifolds placed on both sides of the nosepiece. Typically, the velocity of the hot air is in the range of 0.5 - 0.8 times the speed of sound and the temperature is in the range of 230 - 360 °C. The role of the air streams, first in dragging and attenuating the fibers and then in cooling and laying down the web on the forming table can be evaluated in a number of ways. In this study, the airflow in the nozzle expansion zone is analyzed to identify the effect of the turbulence on the fiber as imposed by the transonic jet. As the turbulence and the mixing layer instabilities play a major role in maintaining a truly transient field, a detailed study was performed using the LES turbulence model to identify flow features in the region immediately downstream of the nozzle. This work highlights the fact that CFD provides an excellent insight into the fast transient phenomena in the air passage during the early stages of fiber formation.

A typical twin slot jet geometry is shown in Figure 9. Dimensions of the jet opening and die-lip are chosen to represent an industrial process. Considering the very large dimension of the die width compared to those of the air-gaps, a two-dimensional study seemed appropriate. Clearly, the small scale eddies will be three-dimensional, as the basic turbulent flow always is. However, in the interest of understanding the large-scale time dynamics, the two-dimensional assumption is appropriate, while the small scale eddies are entirely modeled by the sub-grid scale turbulence model: typically Smagorinsky or RNG model. In the present study we used the RNG sub-grid model. The boundary conditions used are no-slip condition on the die-walls, and atmospheric pressure is used for the pressure-specified and outlet boundaries allowing smooth and free entrainment (inflow) and outflow depending on the internal pressure level. Air is supplied at the inlet with a pressure of 2 atmosphere. Thermal boundary conditions involve specifying temperature at the air-inlet to be 589K or 316°C. The die-walls around the air-slots are considered to be at 566K or 293°C. The horizontal parts of the die-walls are maintained insulated. The atmospheric air temperature is considered to be 300K or 27°C. Along the flow direction, the domain is truncated much earlier than the distance of the forming table with the idea of keeping the problem size reasonable and the pressure boundary condition allows the smooth outflow through this boundary.

The steady state simulation was first carried out with the standard two-equation (k-ε) turbulence model. With this steady state solution, the unsteady mode of simulation was turned on. It was observed that despite using higher order time discretization and time steps as small as 0.1 microseconds, the flow field did not change much and no significant unsteady behavior could be detected. The k-ε turbulence model and its variants are well known to be extra dissipative and such results are fully expected. Figure 10 shows the final results in terms of pressure, turbulent viscosity, temperature and velocity vector plots.

Contrary to the observations with the k-ε turbulence model, the melt-blown die is designed to maintain strong transients. Hence, in the next set of calculation, the LES turbulence model was applied. While using the LES model, the usual procedure is to start the transient simulation with approximate initial pressure, velocity and temperature fields, and continue until a statistically repetitive transient pattern evolves. At that point, the simulation is continued with simultaneous collection of transient statistics for calculation of the mean and rms (Root Mean Square) values of the fluctuating field variables. The simulation needs to be carried out for significantly long period of time. The simulation time is estimated based on the observation of the convection-time for the large eddies present in the flow field. The convection-time is the average time a 'large-eddy' or a vortical structure in the flow-field takes to cross the entire axial distance of the computational domain. Typically, statistics are collected for a few tens of the convection-time scale. It is noted that the average air velocity in the jet may be of the order of 600 m/s but the convection-speed of the large eddies will be significantly lower. The instantaneous flow field itself is very illustrative of the level of turbulence. Figure 11 illustrates an instantaneous snap shot of the flow field. The scales are omitted as the purpose here is to illustrate the large scale eddies present in the flow domain. Also, one can observe a direct correspondence of the various field variables like, pressure, temperature, velocity vectors and the sub-grid scale turbulent viscosity. One of the main features of the flow around the melt-blown die is the issuance of the straight jet from the die-tip. As seen in these figures, the length is approximately one centimeter. Around the tip of this straight jet, the shear layer instabilities have grown strong enough to make the jet begin shedding large scale eddies. The evolution of the alternate shedding eddies is fairly anti-symmetric at this location. But the secondary flow further downstream breaks the pattern and larger scale asymmetry grows. For this particular instant, one can see that most of the shedding eddies have a bias to the right side. At some later instant the pattern changes to the left and the flip-flop continues (unsteady flow-fields with left-bias are not shown here). The temperature contours show streaks of high temperature regions trapped into the large scale eddies and the macro-scale convection of these high-temperature streaks are occurring only at the convection-speed of the large eddies. Close observation of these large eddies further downstream reveals that the high temperature equilibrates within the eddy-structures and it cools down rather slowly even in the presence of strong secondary flows. While the overall length of the current domain is small enough compared to the usual DCD, the large-scale features in close proximity to the die-tip are very influential in controlling the fiber quality. While correlating these observations to the melt-blown fabric manufacturing practices, it is realized that the three important aspects of the process are:

1. The twinjet provides a synchronous pull on the polymer to get the fast attenuation in the immediate vicinity of the die-tip. The polymer is not included in the current simulation and hence no observation could be made on the actual attenuation of fiber dimension. Still, the presence of high temperature and high velocity in the parallel jets is indicative of a favorable environment that can possibly cause the initial attenuation (which is generally a reduction in fiber diameter from ~350 to ~50μm).
2. Significant flow-entrainment takes place around the jet causing shear layer detachment and formation of large scale eddies that provide localized high temperature, high speed air flow causing subsequent attenuation of the fiber diameters. It is conjectured that these large-scale hot eddies result in the generation of the well-known 'log-normal' distribution of the fiber diameters.
3. Subsequent entanglement of the cooled down fibers in further downstream locations is also caused by the relatively slow moving large scale eddies. This aspect will also have significant three-dimensional effects and a corresponding three-dimensional analysis of the flow would refine current observations in terms of the dynamics and statistics.

Another important aspect that remains to be studied further is the effect of the relative motion of the fiber within the jet region. Clearly, air moves faster as long as attenuation is continued in the fiber. But, the shape and size of the fiber strongly influence the drag that determines the strength of the relative motion.

This kind of transient simulation of large eddy structures is powerful enough to provide closer visualization of the flow features and fiber transport scenario. Knowing that the turbulence plays a key role in the melt-blowing process, it would be useful to correlate the observations of the large-scale unsteady features to the level of turbulence in the flow-field using conventional parameters like turbulence intensity and turbulent viscosity. In the context of LES turbulence modeling, the turbulent intensity is calculated through a sequence of analyses. First, the simulation needs to be carried out for a long time (a few convection-time periods) that the so-called 'stationary' state of the flow-field is achieved. A stationary flow-field is a transient ensemble that has a larger time scale of statistically reproducible flow pattern. For jetting flows with strong shear layer instabilities, the transient ensemble involves a large number of eddy sizes and time scales which significantly delays

attainment of the stationary state. The situation in the melt-blowing process is further complicated due to the large amount of low speed secondary air entrainment that introduces a wider range of size and time scales into the domain. Having carried out the simulation for a long span of time, and continuously collecting the mean and fluctuating data for the flow variables, it is possible to describe the time-mean flow-field from an LES study. The mean flow field should be closer to the solution that can be obtained with any conventional RANS model (e.g., k-ε) subject to a fine grid and high order accuracy in the numerical procedure (discretization). On the other hand, the balance of instantaneous and mean quantities characterizes the random turbulent fluctuations. The root mean square (rms) statistics of such quantities indicates the state of turbulence in the field. Figure 12 demonstrates the mean quantities from the current simulation. The mean velocity field indicates that the simulation needs to be carried out for a longer period of time to obtain an exactly symmetric mean field from the instantaneous solutions. The mean pressure field also shows lack of perfect symmetry indicating the need to accumulate further statistics and recompiling the mean.

Figure 13 shows the rms fields for the fluctuations of velocity components and temperature. From the standpoint of explaining the analysis procedure, these figures illustrate how one may identify the rms intensity in the flow field for the velocities and other scalars (e.g., pressure and temperature). While Figures 13a and 13b show the rms fluctuations of the velocity components in the transverse and axial directions respectively, Figure 13c shows the magnitude of the rms of velocity fluctuations. This is the representative of the turbulent kinetic energy (strictly speaking the energy is half the magnitude of the rms vector). The turbulent intensity is the ratio of the turbulent kinetic energy to the mean flow energy. Hence, the turbulent intensity can be derived based on the information contained in Figures 12a and 13c. Once the field map of the turbulent intensity is identified, process parameters like operating pressures, die-opening and forming table distance can be optimized to effectively manipulate the turbulence field and correlate to the fiber attenuation process. It may even be possible to develop further quantitative understanding of the fiber diameter evolution process by more systematic study of these transient turbulent field data. Figure 13d shows the rms fluctuation of the temperature. The region of highest fluctuations in the temperature field is well characterized. This region is one centimeter downstream from the die-tip and about 2 to 3 centimeter long. From previous experimental observation, this region is known to be critically important for birefringence as well as development of diameter distribution. The flow field in the first one-centimeter downstream of the die-tip shows clear distinction from the rest of the jet. This is predominantly the potential core region of the twinjet. The stability, length, temperature and the flow velocity in this region together determine the initial rapid attenuation of the polymer fiber diameter. Thus the LES simulation is found to capture the significant flow features in the melt-blown fabric manufacturing process.

CFD has been used to analyze the flow and heat transfer in the melt-blown fabric manufacturing process. Present study highlighted the limitations of the traditional RANS based turbulence model in capturing the process dynamics. An effective alternative, the Large Eddy Simulation (LES) model is shown to be effective in capturing such dynamics as well as relating back to conventional parameters that measures the level of turbulence in the flow field. This study also paves the way to further analyze the effects of large scale eddies on the size distribution of the melt-blown fabrics.

Simulation of Air Flow and Fiber Accumulation in a Fluff Pad Machine

The fluff pad machine is used to make pads that are used for a variety of personal hygiene products, such as pads and diapers. In modern fluff pad machines, sub-millimeter fiber particles are transported by the turbulent airflow in one or more ducts and are deposited on a rotating wire screen. The distribution of the airflow is the single most important factor determining how fibers are deposited on the screen. Ideally, fibers should be deposited on the screen uniformly, creating homogeneous basis weight. This will happen if: a) the fibers are evenly distributed in the incoming air flow; b) the air flow field is uniform in the vicinity of the screen; and c) the air flow is such, that, once deposited on the screen, fiber particle cannot be carried away. In reality, however, many features of the airflow can prevent this from happening. For example, feeding air ducts have many curves before they reach the screen. Due to inertia, particles may be preferentially concentrated at the end of the curved duct. The turbulent air field may form recirculation zones, stagnation areas or have a pulsating transients. When deposited on the surface, fiber particles create local hydraulic resistance to the airflow. These effects may lead to a non-uniform flow field. Airflow can interact with the spinning screen creating currents along the screen surface. Such currents can blow off loosely deposited particles from the screen. Obviously, clever design of the pad machine must take into account all these and many other factors influencing pad quality. This study shows that CFD offers an opportunity to create a realistic computer model of the flow in the pad machine. As an illustration the model is used to perform a parametric study on the impact of fiber density on the uniformity of the accumulation process. Such model offers an attractive alternative to costly and time consuming prototype testing.

Three transient simulations were run. In the first simulation, the density of the fiber particles was set to a nominal value, 665 kg/m^3. The hydraulic resistance due to the bare screen was included, but the effect of fiber accumulation on the screen resistance was neglected. In the second simulation, the screen resistance increased progressively with fiber accumulation.

The third simulation was similar to the second one except the fact that the density of the fibers was halved. Figure 15a displays the basis weight distribution at the end of the second simulation with nominal fiber density. Since the start time of the particle injection coincided with the initiation of the drum rotation, it took some time for particles to reach the screen. As a result, fiber accumulation is non-uniform in the circumferential direction. Also evident is an axial non-uniformity in the fiber accumulation, with higher values near the wall. The tendency for fibers to collect near the walls is due to fact that the air speed is lower near the wall. So, the drag on the fibers is greater. This increased drag causes more fibers to be drawn into this region. The result is a higher density of slow moving fibers near the wall, and fewer of the fast moving fibers in the free stream area in the middle of the screen. The concentration of particle phase near the wall was also observed in computer simulation of similar particle laden flow in a channel.

Figure 15b displays the basis weight distribution for the third simulation with reduced fiber density. Comparison of Figures 15a and 15b suggests that the maximum basis weight is larger (by a factor of about 1.8) when heavier fibers are used. This is due in part to the fact that the particles in the second simulation are twice as heavy as those in the third simulation. The fact that the ratio is not exactly a factor of 2 is because the number of particles striking the screen governs the increase in hydraulic resistance. Since this number depends on particle density, the combined effect is nonlinear. Also indicated when comparing Figures 15a and 15b, is the tendency for the lighter particles to produce more non-uniformity in the basis weight distribution, and ultimately, pad thickness.

Figure 16 displays the mass flow rate of air in the duct, as a function of time for all the simulations. Fiber particles reach the screen in approximately 0.12 sec, after which the flow rate begins to decrease. Heavier fibers in the second simulation (red) lead to faster flow degradation in comparison to the lighter fibers used in the third simulation (green). The overall decay in the airflow rate for all three simulations is due to the fact that the pad-forming screen is rotating, and in doing so, cutting off the passageway to the outlet holes.

While this study illustrates how CFD can help characterize the transient accumulation process, it is obvious that for a more practically relevant analysis will involve more methodical approach to correlate the rate of accumulation to the growth of hydraulic resistance on the screen surface. Also, the fiber shape and size distribution would play an equally important role in the lay down process as the associated drag law will imply the modification in the near wall flow pattern as well as the accumulation process itself.

Conclusions

In this paper, several computer simulations are showcased to demonstrate the capabilities of CFD to provide insight into the process as well as identify optimum operating conditions for a variety of process parameters. CFD is a very cost-effective and timesaving tool to achieve quick analysis of various process alterations, scale-up and other modification scenario. More importantly, FLUENT's LES turbulence model and Discrete Particle Model are shown to capture process transients in the airflow and fiber-laydown processes.

References

Bresee, R. R. 2001. Understanding The Melt Blowing Process, 2nd Intl. Nonwovens Tech. Conf.. Baltimore, 2001.

Bresee, R.R., and Wadsworth, L.C. September 15-16, 1988. *Book of Papers*. Exxon Melt Blown Seminar. Baytown, Texas,

Fluent Inc. FLUENT 5 user's guide. *Volumes I-V*.

Fox, R. W. And Kline, S. J. 1962. "Flow Regimes in Curved Subsonic Diffusers." *Journal of Basic Engineering*. Vol. 84, Sept. 1962, pp. 303-312.

Goswami, B.C. 1997. Spunbounding and melt-blowing processes, in *Manufactured Fiber Technolgy*, Edited by Gupta, V.B. and Kothari, V.K., Chapman & Hall, London.

Mathur, S.R., and Murthy, J. Y. 1997. A Pressure Based Method for Unstructured Meshes." *Numerical Heat Transfer*. Vol. 31, pp. 195-216.

Mukhopadhyay, A., R.O.S. Prasad, E. Grald, J. Sun, and N. Lifshutz. 2001. Performance Analysis of Melt-blown Dies Using Computational Fluid Dynamics, 2nd INTC Conference, Baltimore.

Mizua, T. and Kasagi, N. 1998. Numerical analysis of particle motion in turbulent channel flow. CD ROM Publication in *Proceedings of Third International Congress on Multiphase Flow, ICMF'98*. June 8-12, Lyon, France.

Prasad, R.O.S. and Runstadler, P.W. 2001. Proceeding of the INTC Conference. September 26-28, Dallas, TX, USA, pp.13.1-13-16.

Troshko, A., Sun, J. and Grald, E. 2001. Computer Analysis of Air Flow and Fiber Accumulation in a Fluff Pad Machine, 2nd INTC Conference, Baltimore, 2001.

White C. March 2000. Nonwovens Training Course Material, INDA.

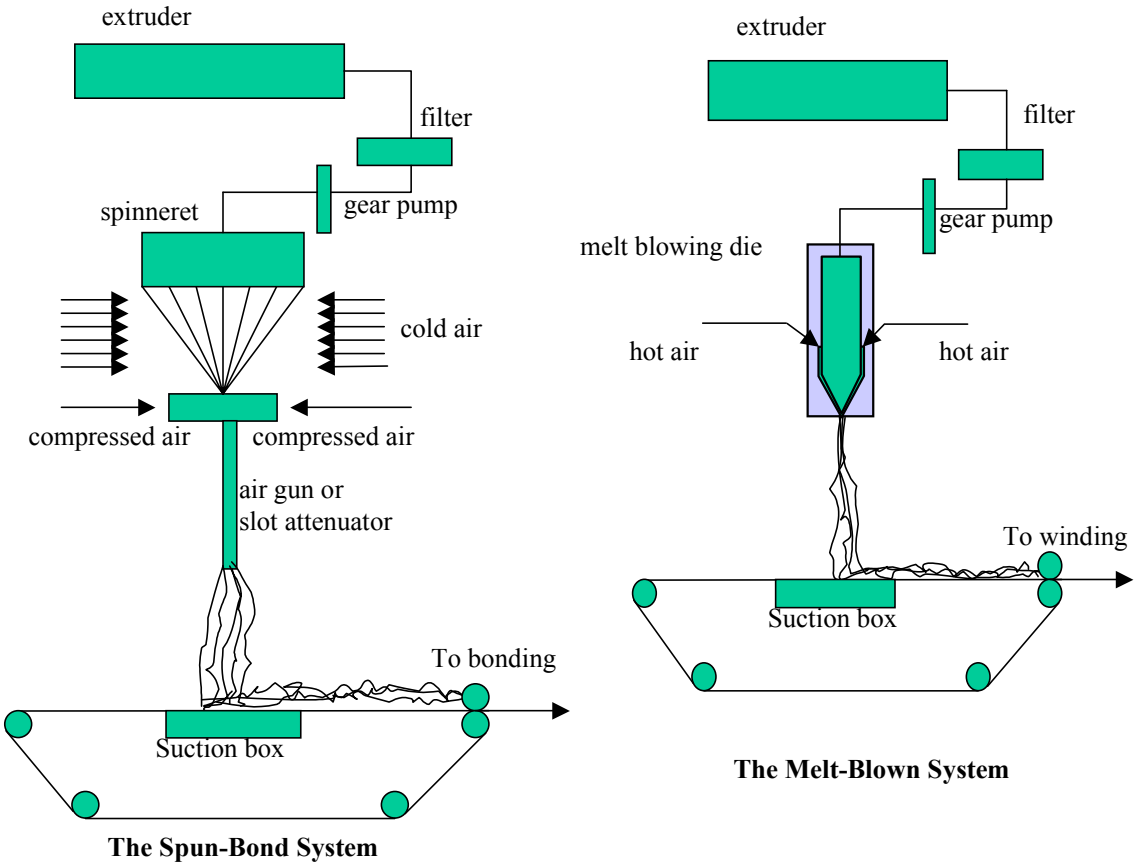

Figure 1. Spun-bonding and melt-blowing processes for nonwoven fabric manufacturing.

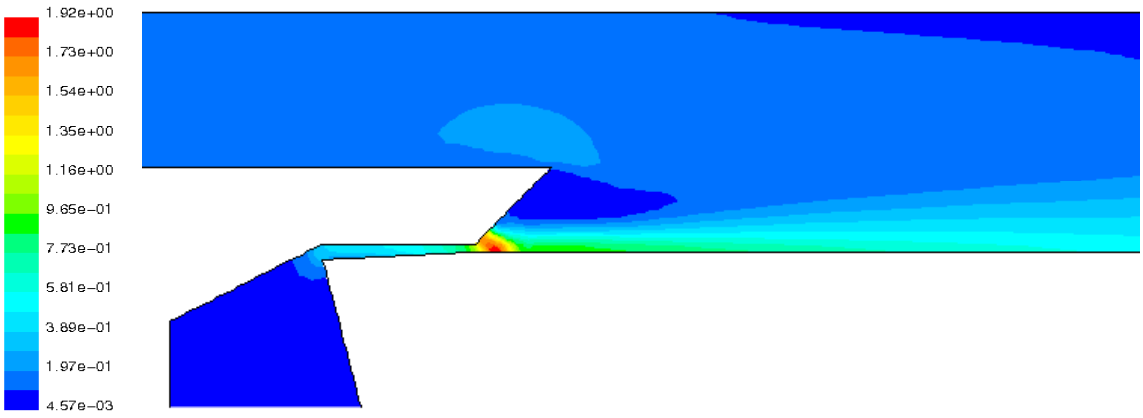

Figure 2. Contours of Mach Number in the Primary Airflow System.

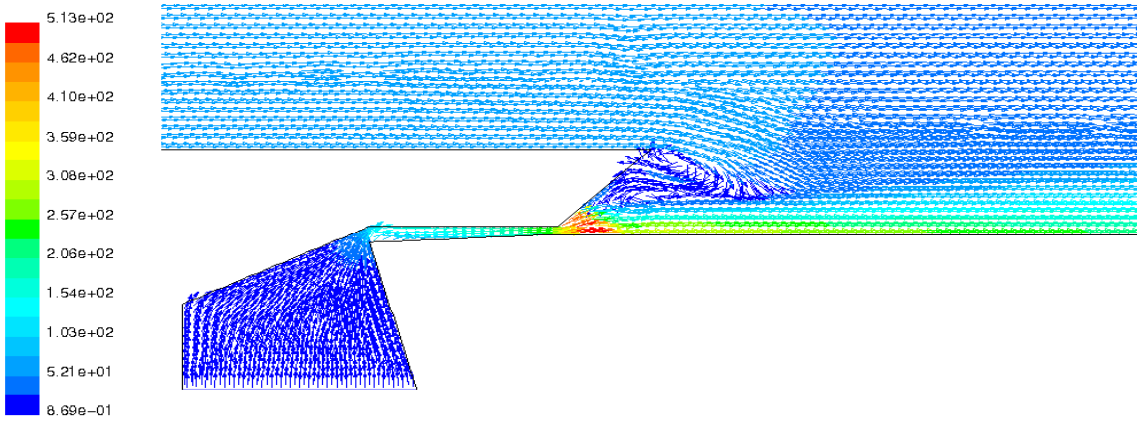

Figure 3. Velocity Vectors in the Primary Airflow System.

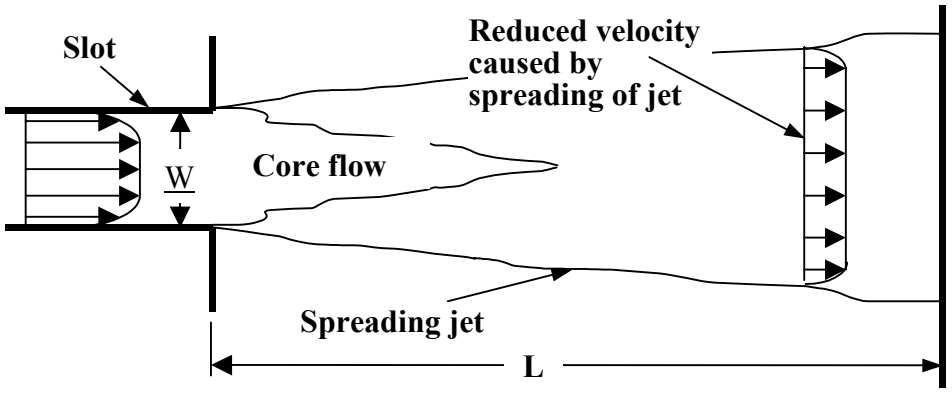

Figure 4. Turbulent Spreading of an Unconfined Jet.

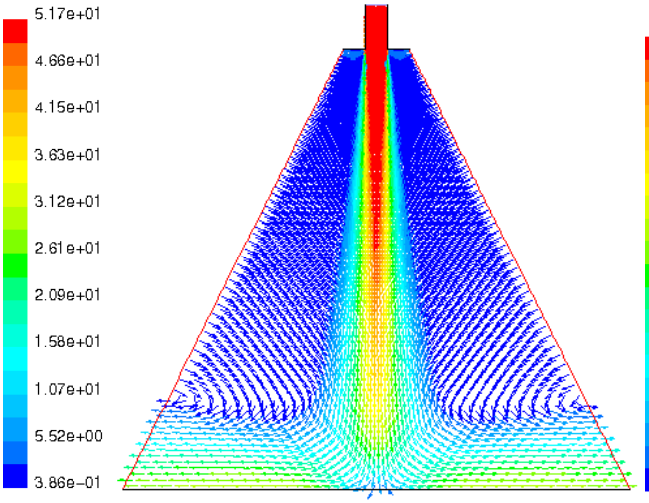

Figure 5. Time-Average Velocity Vectors in a Planar Turbulent Jet.

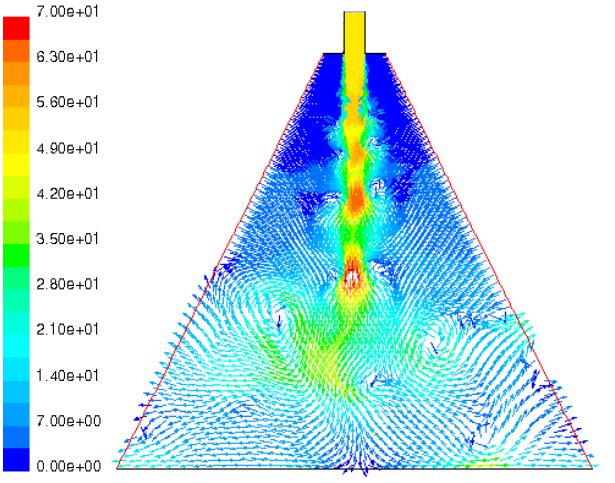

Figure 6. Instantaneous Velocity Vectors in a Planar Turbulent.

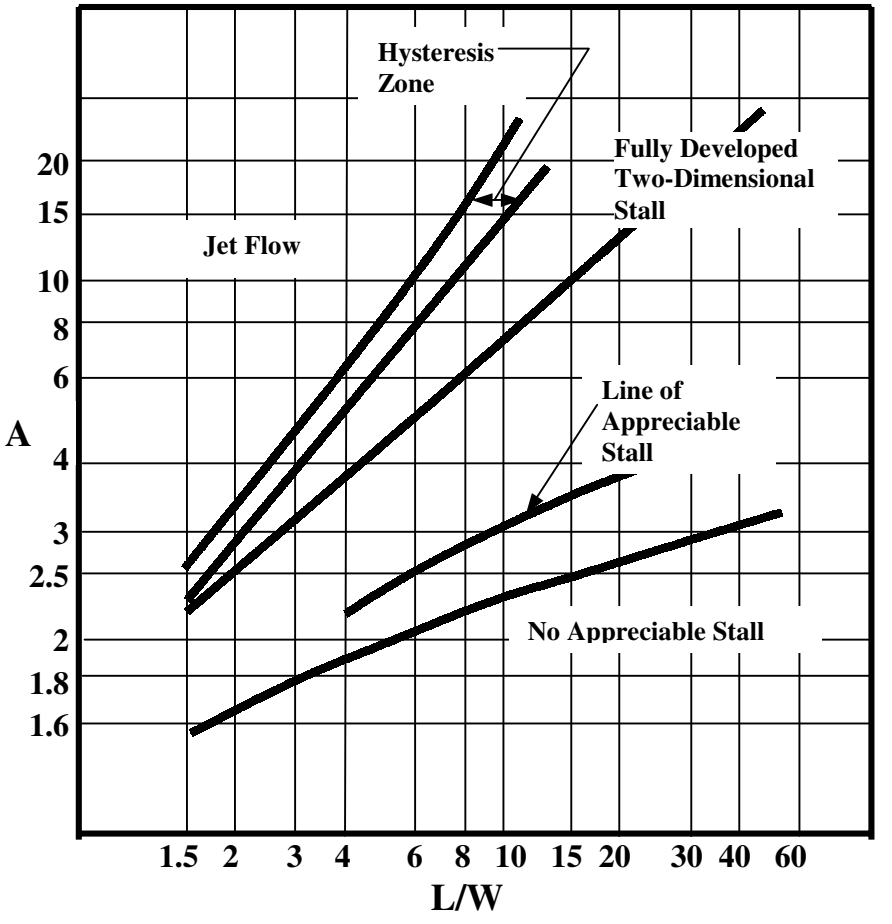

Figure 7. Diffuser Flow Regime Map (Fox and Kline, 1962).

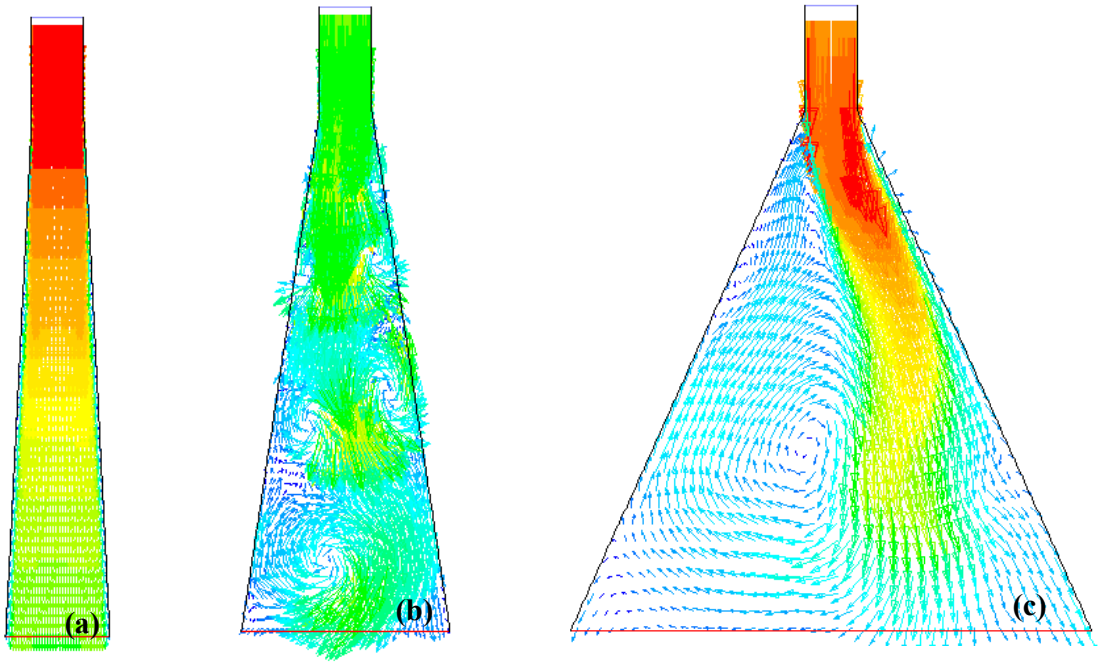

Figure 8. Flow field in different diffusers: (a) an Unstalled Diffuser; (b) a Diffuser with Transient Stall Conditions; (c) a Diffuser with Fully Stalled Conditions.

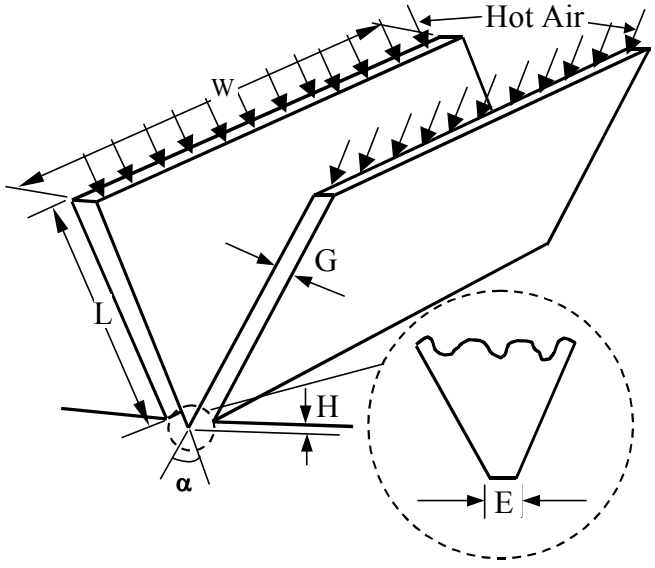

Dimension	Value
L	0.65 cm
W	25 cm
G	0.038 cm
H	0.0127 cm
E	0.005 cm
α	60 deg

Figure 9. The geometry and the dimensions of the melt-blown die. Note that the actual air slot length (L) can be much longer. A truncated slot part is used for this study.

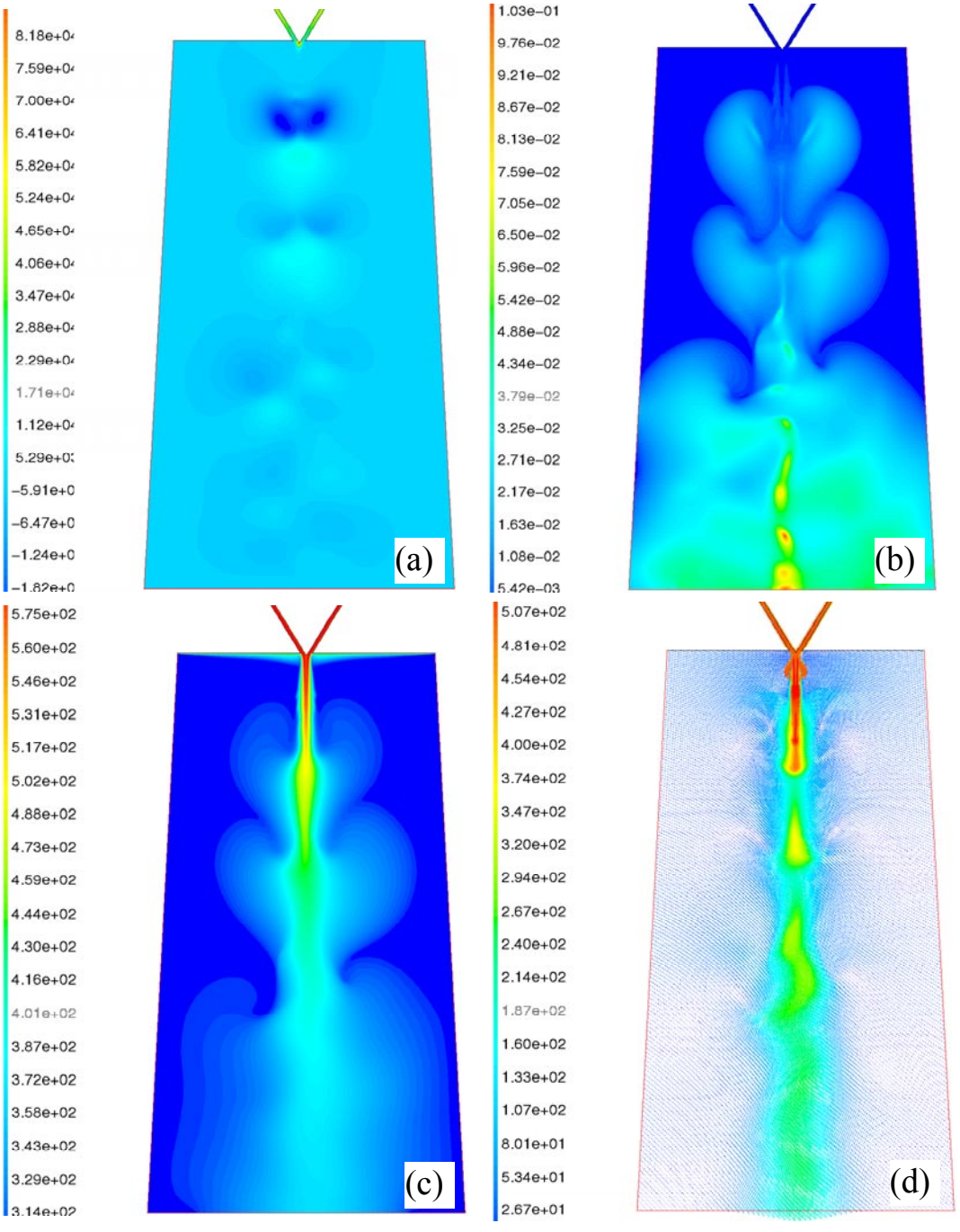

Figure 10. Predicted steady state in unsteady calculation with k-ε turbulence model: (a) pressure; (b) turbulent viscosity; (c) temperature and (d) velocity vectors.

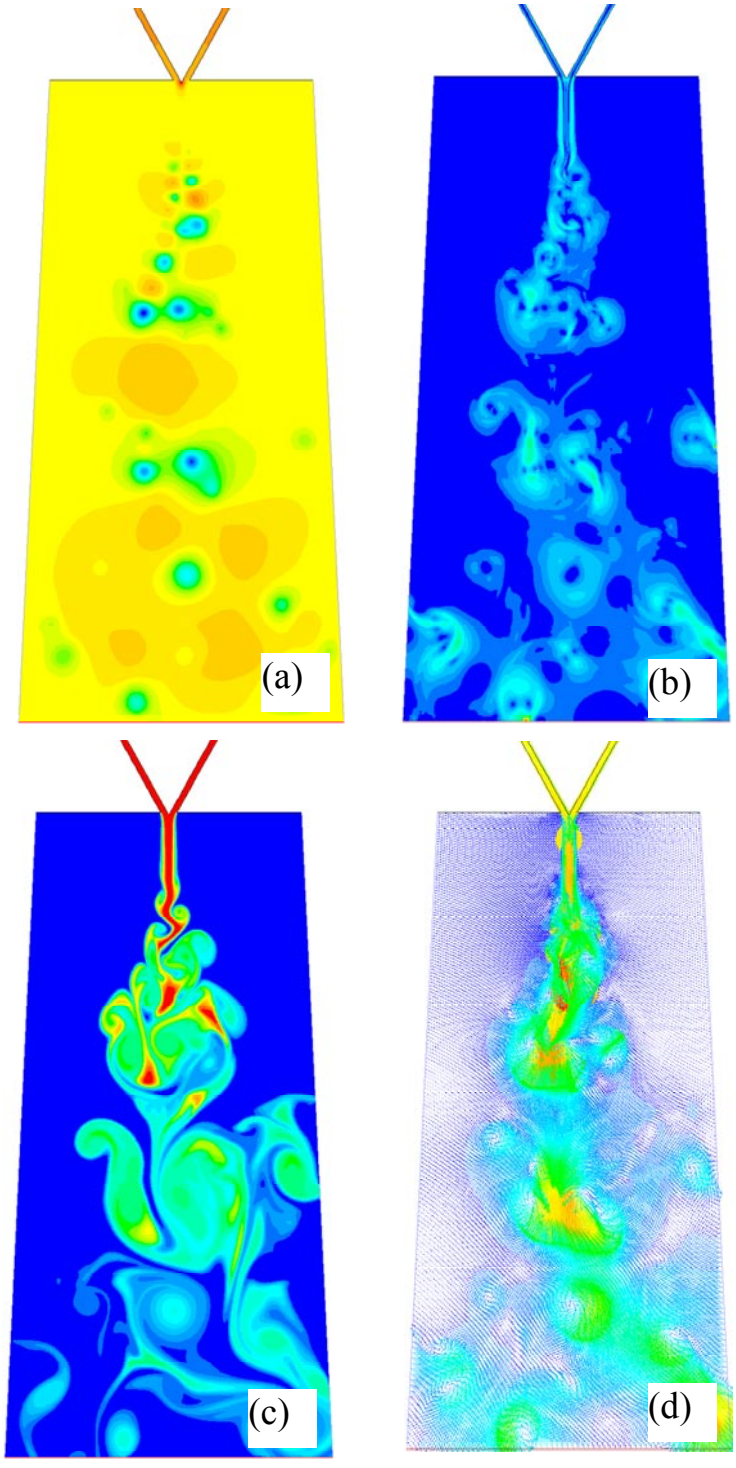

Figure 11. Instantaneous flow fields with LES; (a) pressure; (b) Sub-grid-scale eddy viscosity (kg/ms) (c) temperature(°C); (d) velocity vectors (m/s).

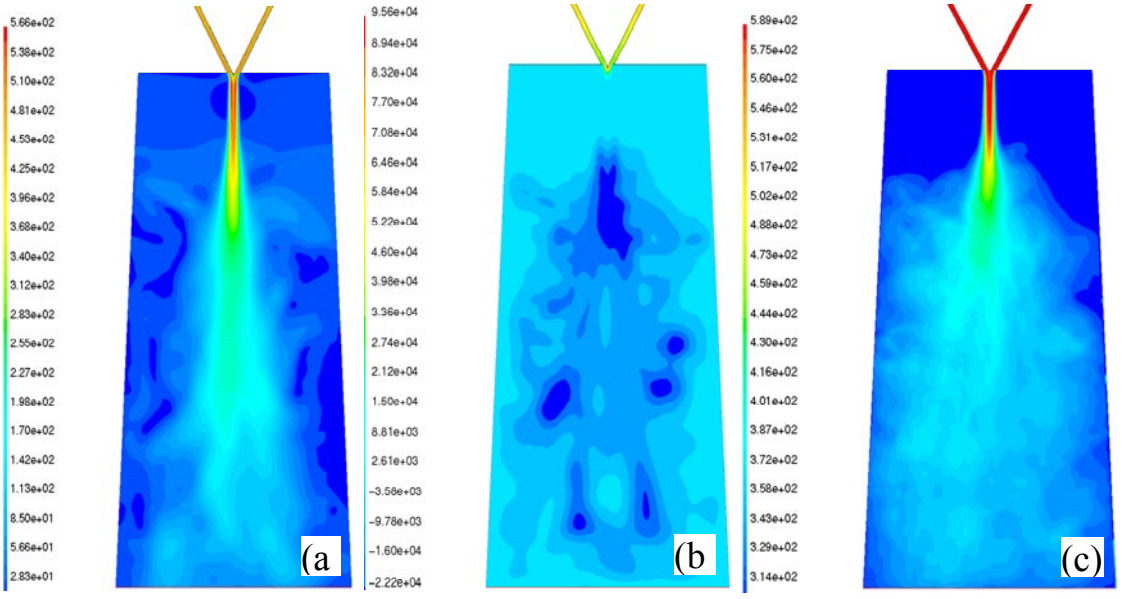

Figure 12. Time average (mean) flow field from LES simulation; (a) velocity magnitude (m/s); (b) static pressure (Pa); (c) temperature (°C).

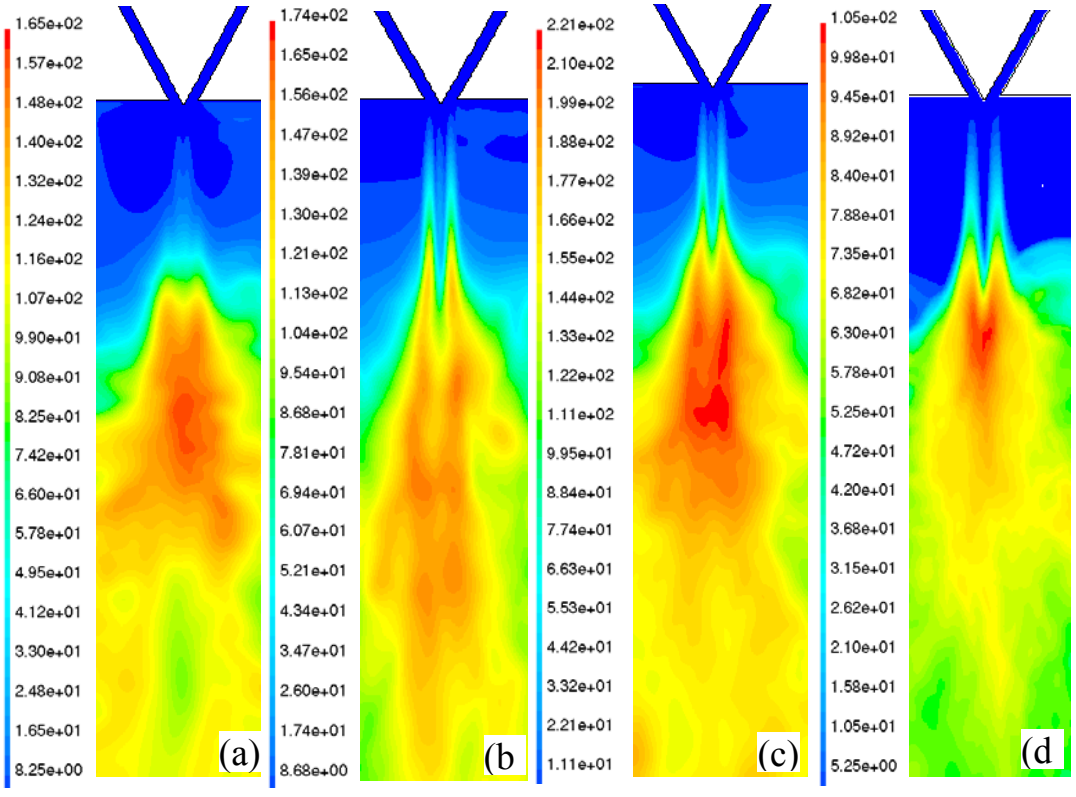

Figure 13. RMS values of flow field fluctuations: (a) transverse velocity component (m/s); (b) axial velocity component (m/s); (c) velocity magnitude (m/s) and (d) temperature (°C).

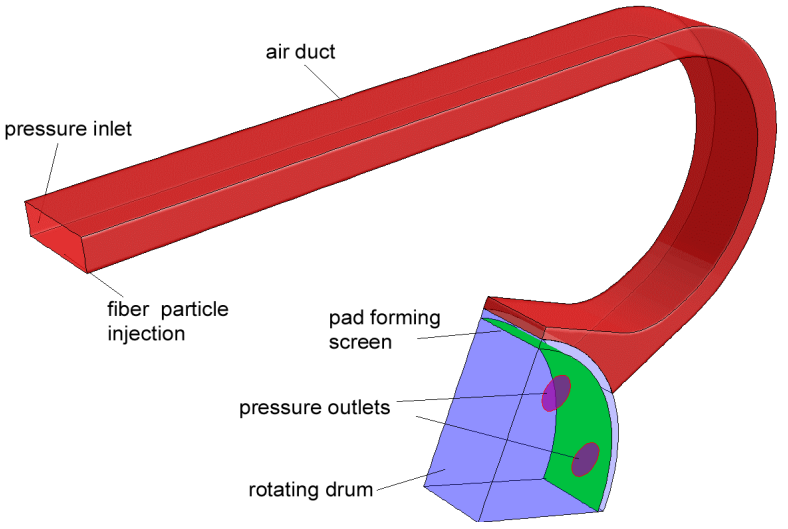

Figure 14. Part of the diaper-making machine modeled with CFD.

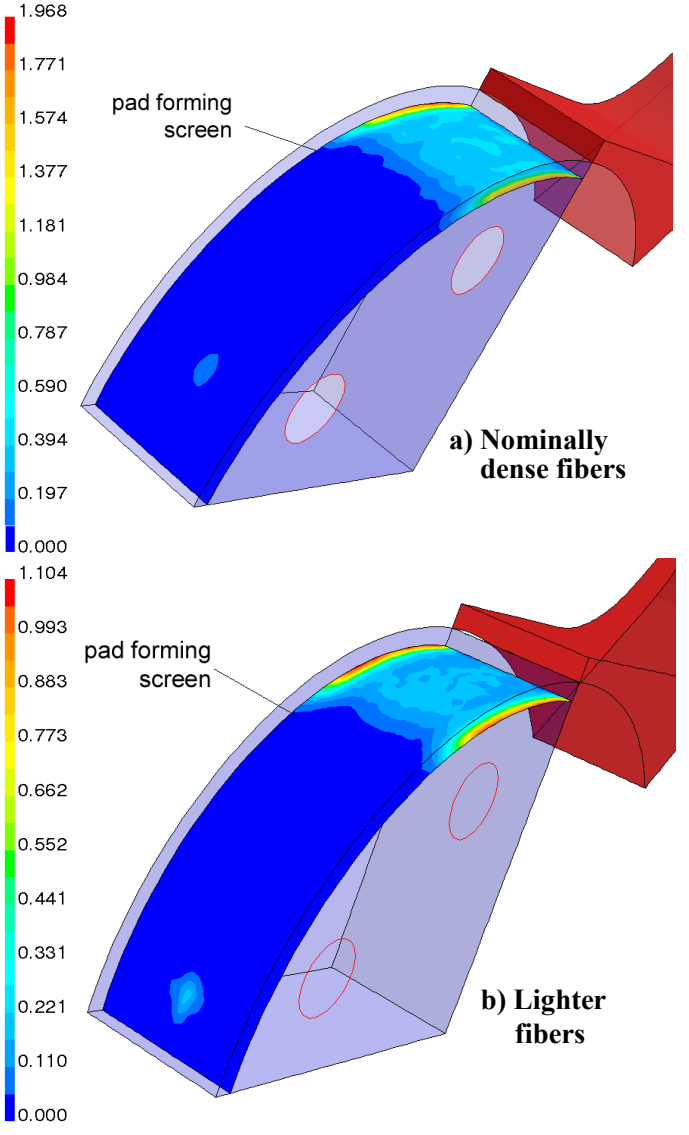

Figure 15. Basis weight distribution (kg/m$^{2)}$ for (a) nominal and (b) light particles.

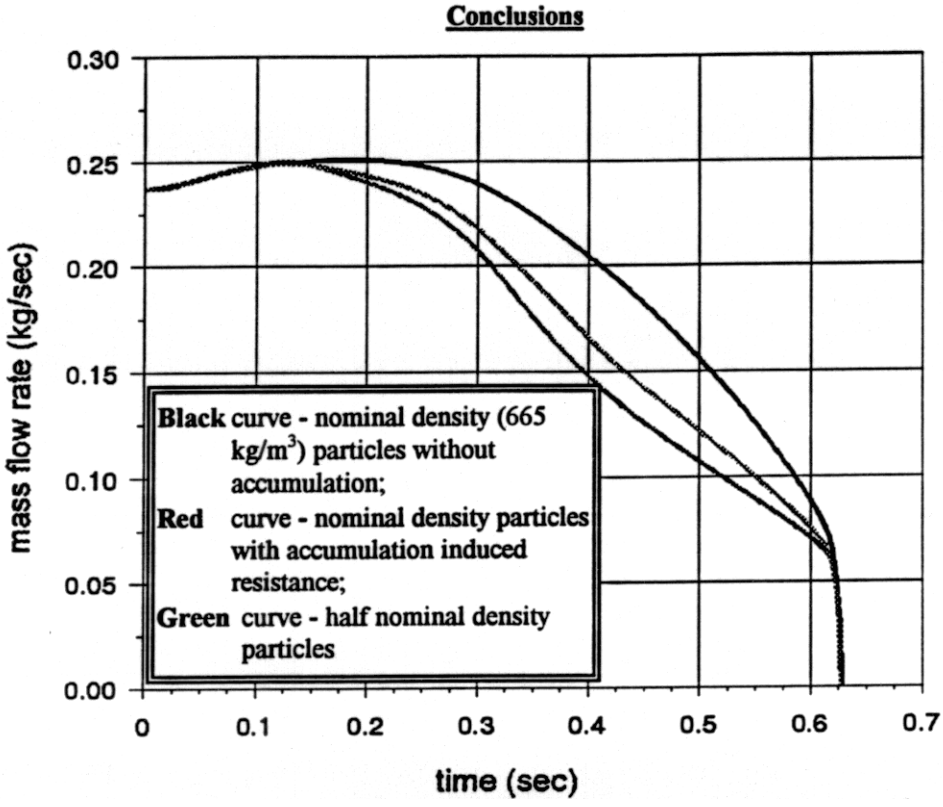

Figure 16. Air mass flow rate (kg/s) vs. time (s) on the fluff pad machine screen.